

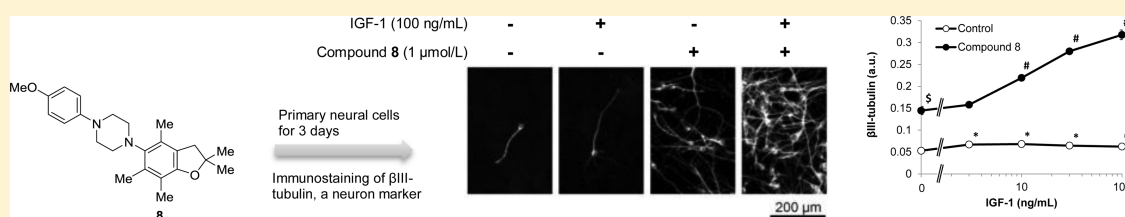
Discovery of Benzofuran Derivatives that Collaborate with Insulin-Like Growth Factor 1 (IGF-1) to Promote Neuroprotection

Takeshi Wakabayashi,^{*,†} Norihito Tokunaga,[†] Kazuyuki Tokumaru,[†] Taiichi Ohra,[†] Nobuyuki Koyama,[‡] Satoru Hayashi,[†] Ryuji Yamada,[†] Mikio Shirasaki,[†] Yoshitaka Inui,[†] and Tetsuya Tsukamoto[†]

[†]Pharmaceutical Research Division, Takeda Pharmaceutical Company, Ltd., 26-1 Muraoka-Higashi 2-chome, Fujisawa, Kanagawa 251-8555, Japan

[‡]Japan Oncology Business Unit, Takeda Pharmaceutical Company, Ltd., 12-10, Nihonbashi 2-chome, Chuo-ku, Tokyo 103-8668, Japan

Supporting Information



ABSTRACT: A series of benzofuran derivatives with neuroprotective activity in collaboration with IGF-1 was discovered using a newly developed cell-based assay involving primary neural cells prepared from rat hippocampal and cerebral cortical tissues. A structure–activity relationship study identified compound **8** as exhibiting potent activity and brain penetrability. An in vitro pharmacological study demonstrated that although IGF-1 and **8** individually exhibited the neuroprotective effect, the latter acted in collaboration with IGF-1 to enhance neuroprotective activity.

INTRODUCTION

Insulin-like growth factor 1 (IGF-1) is a growth hormone with structural and functional homologies to IGF-2 and insulin. IGF-1 exerts its pleiotropic effects via the activation of an intracellular signaling system, such as phosphatidylinositol 3-kinase (PI3K)/Akt pathway, through binding to its receptor.¹ IGF-1 and insulin play an important role in the regulation of physiological functions such as glucose metabolism.² IGF-1 also has important functions in the brain, including metabolic, neurotrophic, neuromodulatory, and neuroendocrine actions.^{3,4} Reportedly, IGF-1 can promote the survival, proliferation, and maturation of cultured neurons,⁵ reduce neuronal loss in adult rat brains following a hypoxic–ischemic injury,⁶ induce the differentiation of oligodendrocytes,⁷ stimulate DNA synthesis⁸ and neurite outgrowth,⁹ direct the sprouting of spared afferents into a deafferented hippocampus,¹⁰ modulate hippocampal acetylcholine release,¹¹ reduce phosphorylation of tau protein,¹² protect hippocampal neurons against the toxicity of β -amyloid protein ($A\beta$), and directly affect the metabolism and clearance of $A\beta$.¹³ Given these findings, small molecules that collaborate with IGF-1 to enhance the IGF-1 action would be potentially useful for the treatment of central nervous system (CNS) disorders such as brain ischemia and Alzheimer's disease (AD).

We have developed a cell-based assay to evaluate the collaborative effect with IGF-1 using primary neural cells prepared from rat hippocampal and cerebral cortical tissues, where cell death is induced by serum starvation and neuronal survivability in the presence of IGF-1 is estimated by

immunoreactivities of β III-tubulin, a marker of immature neurons, using the cell-enzyme-linked immunosorbent assay (ELISA) system. On the basis of the fact that serum deprivation decreases cell survival in cortical cultures, the increase in the number of β III-tubulin positive cells in this experiment is presumed to show a neuroprotective effect. Compound screening of our chemical library with this novel phenotype assay resulted in our discovery of a series of hit compounds with several different chemotypes. Subsequent hit-to-lead activities were conducted on the basis of CNS drug-like properties suggested in the literature,¹⁴ which culminated in the identification of benzofuran-3-one **1a** as a lead compound (Figure 1). While both IGF-1 and **1a** promoted neuroprotection in this assay, cotreatment with IGF-1 and **1a** further enhanced it in a collaborative manner, where the EC_{50} value of **1a** was 0.12 μ M. The neuroprotective effect is described in

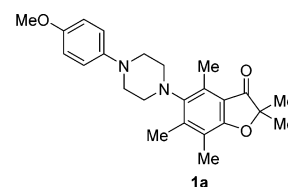


Figure 1. Structure of **1a**.

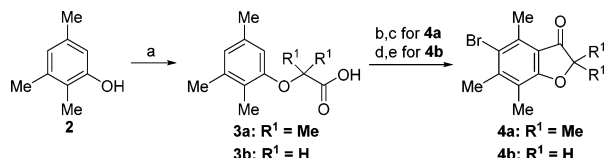
Received: February 5, 2016

detail later. With the lead molecule **1a** in hand, we initiated medicinal chemistry efforts aimed at not only uncovering structure–activity relationships (SARs) but also developing a potential drug candidate. This report describes the synthesis and neuroprotective activity of the derivatives of benzofuran **1a**.

CHEMISTRY

The synthesis of **1a** and related compounds is outlined in Schemes 1–6. Scheme 1 shows the preparation of the key intermediary bromides **4a,b**.

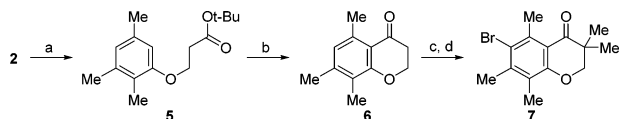
Scheme 1. Synthesis of Compounds **4a,b**^a



^aReagents and conditions: (a) BrC(R¹)₂CO₂H, NaOH, MEK, 50 °C; (b) PPA, 70 °C; (c) Br₂, AcOH, rt; (d) (i) (COCl)₂, DMF, THF, 0 °C–rt, (ii) AlCl₃, CH₂Cl₂, –78 °C–rt; (e) NBS, MeCN, rt.

O-Alkylation¹⁵ of phenol **2** and the successive intramolecular Friedel–Crafts-type acylation of the resulting propionic acid **3a,b** yielded benzofuran-3-ones, which were brominated to form **4a,b**. In these transformations, polyphosphoric acid (PPA) and bromine/acetic acid (AcOH) were used for the synthesis of **4a**. However, these reagents were observed to be inapplicable for the synthesis of **4b** because of its relatively unstable nature against acidic media. Compound **4b** was thus prepared under relatively mild conditions comprising acid chloride formation followed by treatment with aluminum chloride and successive bromination with *N*-bromosuccinimide (NBS). Bromide **7**, a key intermediate for the chromane derivative, was synthesized according to Scheme 2.

Scheme 2. Synthesis of Compound **7**^a

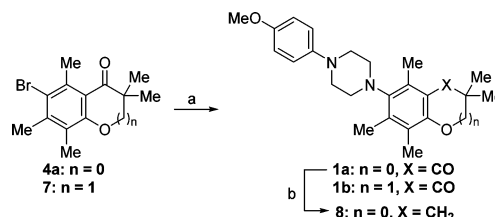


^aReagents and conditions: (a) *tert*-butyl acrylate, KO*t*-Bu, 130 °C; (b) PPA, 100 °C; (c) MeI, KO*t*-Bu, THF, –78 to 60 °C; (d) NBS, MeCN, rt.

Chromane **6** was prepared from **2** in a manner similar to the preparation of the benzofuran-3-one, i.e., O-alkylation by Michael addition with *tert*-butyl acrylate and the PPA-promoted cyclization of the resulting *tert*-butyl ester **5**. After 3,3-dimethylation of **6**, bromination with NBS produced **7**. Buchwald coupling of 4-methoxyphenylpiperazine with **4a** and **7** using palladium acetate and 2,2'-bis-(diphenylphosphino)-1,1'-binaphthyl (BINAP) proceeded to form compounds **1a** and **1b**, respectively. Furthermore, alane reduction of **1a** furnished dihydrobenzofuran **8** (Scheme 3).

With respect to **11**, the 3-carbonyl group of the coupling precursor **4b** was protected by treatment with *tert*-butyldimethylsilyl trifluoromethanesulfonate (TBSOTf) and triethylamine (Et₃N)¹⁶ and the protecting group was removed with HCl after the Buchwald coupling. The alane reduction of **10** gave a crude product of the desired dihydrobenzofuran **11**

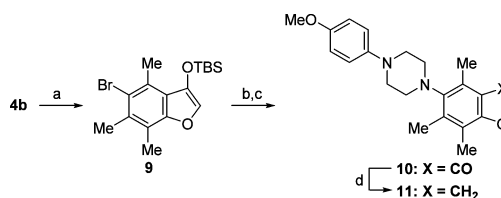
Scheme 3. Synthesis of Compounds **1a,b** and **8**^a



^aReagents and conditions: (a) 1-(4-methoxyphenyl)piperazine, palladium acetate, BINAP, NaO*t*-Bu, toluene, reflux; (b) LiAlH₄, AlCl₃, THF, reflux.

contaminated with the corresponding benzofuran, which was hydrogenated directly to form pure **11** (Scheme 4).

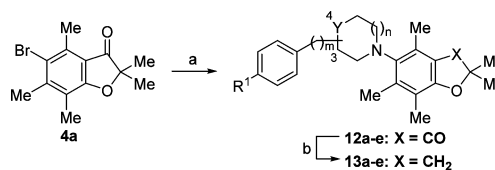
Scheme 4. Synthesis of Compound **11**^a



^aReagents and conditions: (a) TBSOTf, Et₃N, toluene, 0 °C–rt; (b) 1-(4-methoxyphenyl)piperazine, palladium acetate, BINAP, NaO*t*-Bu, toluene, reflux; (c) HCl, THF, rt; (d) (i) LiAlH₄, AlCl₃, THF, reflux, (ii) H₂, Pd/C, EtOAc, 60 °C.

Dihydrobenzofurans **13a–e** bearing a 2,2-dimethyl group were prepared from the intermediary bromide **4a** and corresponding piperazine or morpholin derivatives in the same manner as the preparation of **8** (Scheme 5).

Scheme 5. Synthesis of Compound **13a–e**^a

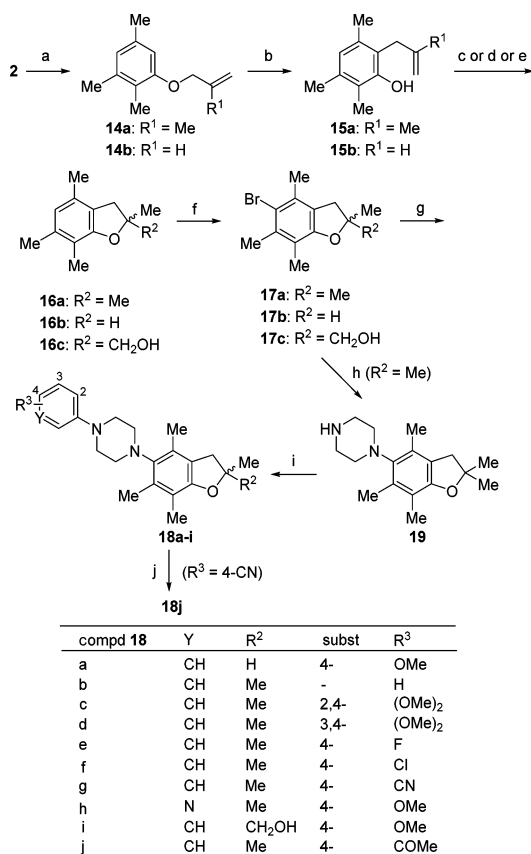


compd 12 and 13	n	m	subst	Y	R ¹
a	1	1	4-	N	OMe
b	2	0	4-	N	OMe
c	1	0	3-	O	OMe
d	1	0	3-	NMe	OMe
e	1	0	4-	N	Me

^aReagents and conditions: (a) amine, palladium acetate, BINAP, NaO*t*-Bu, toluene, reflux; (b) LiAlH₄, AlCl₃, THF, reflux.

Scheme 6 shows an alternative synthetic route for the dihydrobenzofuran derivatives.¹⁷

O-Alkylation of **2** followed by Claisen rearrangement formed **15a,b**. The treatment of **15a** with *p*-toluenesulfonic acid (*p*-TsOH) or *m*-chloroperoxybenzoic acid (*m*CPBA) formed **16a** or **16c**, respectively, whereas the treatment of **15b** with HCl formed **16b**. After bromination, **17a–c** were converted to **18a–i** directly or in a three-step manner via **19**. In the case of **18a** and **18i**, the optical resolution of the racemic form was performed by chiral high-performance liquid chromatography (HPLC) to give both enantiomers, i.e., (*R*)- and (*S*)-**18a,i**. In

Scheme 6. Synthesis of Compound 18a–j^a

^aReagents and conditions: (a) CH₂ = C(R¹)CH₂Br, K₂CO₃, DMF, 100 °C; (b) PhNEt₃, 210 °C; (c) *p*-TsOH, toluene, reflux for **16a** from **15a**; (d) HCl, EtOH, reflux for **16b** from **15b**; (e) (i) *m*CPBA, toluene, rt, (ii) TFA, toluene, rt for **16c** from **15a**; (f) NBS, MeCN, rt; (g) *N*-arylpiperazine, palladium acetate, BINAP, NaOt-Bu, toluene, reflux or microwave, 160 °C, (chiral HPLC for (*R*)- and (*S*)-**18a,i**); (h) (i) 1-(*tert*-butoxycarbonyl)piperazine, palladium acetate, BINAP, NaOt-Bu, toluene, reflux, (ii) HCl, EtOAc, 50 °C; (i) aryl bromide, palladium acetate, BINAP, NaOt-Bu, toluene, microwave, 150 °C; (j) MeLi, THF, 0 °C.

addition, the reaction of nitrile **18g** with methyl lithium (MeLi) produced ketone **18j**.

RESULTS AND DISCUSSION

A pharmacokinetic study of **1a** revealed that it exhibited oral bioavailability (BA: 42.3%) and brain penetrability in rats (brain/plasma concentration ratio (K_p) was 3.4 at 1 h after intravenous (iv) administration). However, it was later observed to exhibit strong CYP2C9 inhibitory activity and phototoxicity (Table 1). Compound **1a** structurally comprises three parts: a benzofuran scaffold, piperazine linker, and terminal aryl group. We assumed that the benzofuran-3-one scaffold would be responsible for the aforementioned two issues for the following two reasons. First, analysis with MetaSite,¹⁸ a computational procedure that predicts metabolic transformations related to cytochrome-mediated reactions during phase I metabolism, suggested that the carbonyl group of the scaffold would largely contribute to the binding of **1a** with CYP2C9 enzyme at a transition state of the metabolism. Second, the benzofuran-3-one scaffold is characterized by a highly planar, cyclic, conjugated π -electron system that may be

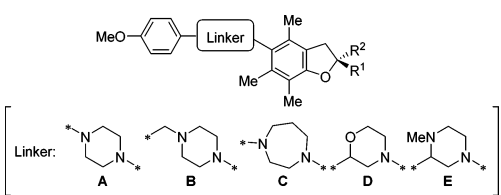
Table 1. Neuroprotective Activity, CYP2C9 Inhibitory Activity, and Phototoxicity of Compounds **1a,b** and **8**

compd	neuroprotection ^a EC ₅₀ (μM)	CYP2C9 inhibition ^b (%)	phototoxicity MPE ^c
1a	0.12 (0.10–0.14)	83.4	0.231
1b	0.51 (0.48–0.54)	42.1	NT ^d
8	0.15 (0.13–0.20)	–0.9	–0.049

^aNeuroprotective activity with primary neural cultures in the presence of IGF-1 (100 ng/mL) is exhibited. EC₅₀ values are shown with 95% confidence intervals given in parentheses ($n = 3–5$). ^bPercent inhibition at 10 μM is exhibited. ^cMPE (mean photo effect) was calculated with a software package (Phototox version 2.0).²⁰ ^dNot tested.

linked to phototoxicity.¹⁹ Thus, in our SAR study, we first examined the modification of the scaffold in the following two ways: the expansion of the 5-membered furan ring to a 6-membered pyran ring and removal of the carbonyl group of the scaffold. With respect to chromane **1b**, whose carbonyl group takes a conformation that slightly differs from that of **1a**, the CYP2C9 inhibitory effect was moderately improved, as expected; however, the neuroprotective activity was reduced approximately 4-fold. In contrast, dihydrobenzofuran **8** exhibited neither CYP2C9 inhibition nor phototoxicity while maintaining its potent neuroprotective activity. These results are consistent with our hypothesis that the adverse effects of **1a** would be influenced by the modification of the benzofuran-3-one scaffold and removal of the carbonyl group, representing an effective approach. In addition, the carbonyl group was determined to not be essential for the neuroprotective activity. Considering these results, the 2,3-dihydro-1-benzofuran ring was chosen as the scaffold for the subsequent SAR study.

The SAR of the substituent on the 2-position of the dihydrobenzofuran ring and linker is summarized in Table 2. Deletion of the 2-methyl group of **8** (**11**, (*S*)- and (*R*)-**18a**) caused a slight loss in activity, and the introduction of a hydroxy group ((*S*)- and (*R*)-**18i**) induced a decrease that was more than 4-fold, suggesting that a lipophilic group would be favored as the 2-substituent. The stereochemistry of **18a** and **18i** appears to be unrecognized in this assay. With respect to the linker moiety between the benzofuran scaffold and the terminal aryl group, the insertion of a methylene group between the side benzene ring and piperazine (**13a**) caused a more than 4-fold reduction in activity compared with that of **8**. Expansion from a 6- to a 7-membered ring (**13b**) slightly enhanced the potency, suggesting that a vector of the terminal phenyl group of **13b** would be slightly more suitable. Further change in the vector was detrimental because compounds **13c** and **13d**, with a more bent molecular framework resulting from the terminal aryl group attached in a different manner, exhibited a significant decrease in activity compared with **13b**. Overall, the results indicate that piperazine derivative **8** and homopiperazine derivative **13b** exhibited relatively greater activity. In the meantime, the metabolic clearance of **13b** with human liver microsome was observed to be markedly faster compared with that of compound **8** (**13b**, 87 μL/min/mg; **8**, 2 μL/min/mg). This difference in metabolic clearance might be due to the conformationally flexible homopiperazine moiety of **13b**, which

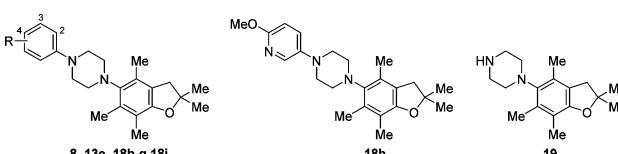
Table 2. Neuroprotective Activity of Compounds 8, 11, 13a–d, and 18a,i


compd	R ¹	R ²	linker	neuroprotection ^a EC ₅₀ (μM)
8	Me	Me	A	0.15 (0.13–0.20)
11	H	H	A	0.23 (0.21–0.26)
(S)-18a	H	Me	A	0.46 (0.37–0.55)
(R)-18a	Me	H	A	0.44 (0.35–0.59)
(S)-18i	CH ₂ OH	Me	A	0.70 (0.67–0.74)
(R)-18i	Me	CH ₂ OH	A	0.63 (0.57–0.68)
13a	Me	Me	B	0.68 (0.54–0.84)
13b	Me	Me	C	0.076 (0.065–0.088)
13c ^b	Me	Me	D	0.37 (0.34–0.41)
13d ^b	Me	Me	E	0.55 (0.47–0.64)

^aNeuroprotective activity with primary neural cultures in the presence of IGF-1 (100 ng/mL) is exhibited. EC₅₀ values are shown with 95% confidence intervals given in parentheses ($n = 3–5$). ^bRacemate.

is consistent with empirical observations indicating that flexible molecules tend to be metabolically unstable.²¹ Accordingly, the original piperazine linker A was chosen for further SAR studies.

We next investigated the terminal aryl group (Table 3). As shown in the bottom row of the table, the intermediary

Table 3. Neuroprotective Activity of Compounds 8, 13e, 18b–h,j, and 19


compd	R	neuroprotection ^a EC ₅₀ (μM)
8	4-OMe	0.15 (0.13–0.20)
13e	4-Me	0.13 (0.12–0.15)
18b	H	0.38 (0.28–0.52)
18c	2,4-diOMe	0.39 (0.36–0.44)
18d	3,4-diOMe	0.27 (0.22–0.32)
18e	4-F	0.30 (0.28–0.33)
18f	4-Cl	0.66 (0.51–0.92)
18g	4-CN	>1.0
18h		0.62 (0.55–0.69)
18j	4-COMe	0.15 (0.14–0.18)
19		(20% @ 10 μM)

^aNeuroprotective activity with primary neural cultures in the presence of IGF-1 (100 ng/mL) is exhibited. EC₅₀ values are shown with 95% confidence intervals given in parentheses ($n = 3–5$).

piperazine derivative 19, lacking the terminal *p*-methoxyphenyl group, exhibited very weak potency, suggesting that the aryl group might be essential for the activity. We thus focused on the modification of a substituent on the benzene ring or replacement with a heteroaryl ring. The substitution of a methyl group (13e) for the methoxy group of 8 resulted in a compound with comparable activity, whereas the removal of the methoxy group (18b) from the benzene ring induced a

slight decrease in activity, suggesting that substitution at the 4-position of the benzene ring is important for the activity. The introduction of an additional methoxy group at the 2- or 3-position of 8 (18c,d) caused a slight loss of activity, which led us to focus on 4-monosubstituted derivatives. With respect to the substitution of a halogen atom, 4-fluoro derivative 18e exhibited comparable activity with that of nonsubstituted derivative 18b, whereas 4-chloro derivative 18f was slightly less potent than 18e. 4-Cyano derivative 18g exhibited weak potency and methoxypyridine derivative 18h exhibited an about 4-fold decrease in activity compared with that of 8; however, 4-acetyl derivative 18j exhibited recovered potency comparable with that of 8. In conclusion, these results indicate that the substitution of the 4-methoxy (8), 4-methyl (13e), and 4-acetyl (18j) groups are highly beneficial for the activity, although the SAR is not fully understood; this lack of understanding is at least partly attributable to the cell-based assay that we employed, where the activity is determined by multiple factors.

The neuroprotective effect of 8 is exhibited in detail in Figures 2 and 3. The cells were cultivated in a serum-free

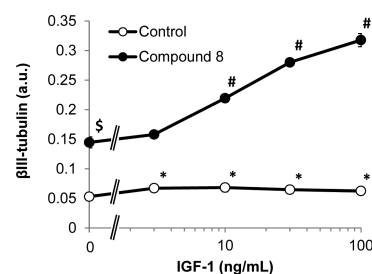


Figure 2. Neuroprotective effect of 8 in rat primary neural cells. After a 4-day culture in a serum-containing medium, the cells were cultivated in a serum-free medium for 3 days in the absence or presence of IGF-1 and 1 μmol/L 8. The number of neurons was estimated using a cell-ELISA system detecting βIII-tubulin, a neuron marker. Compound 8 and IGF-1 exhibited a protective effect on neuron. Data represent mean ± SEM of four wells. * $p \leq 0.025$ versus Control without IGF-1 (one-tailed Shirley–Williams' test). # $p \leq 0.025$ versus 8 without IGF-1 (one-tailed Williams' test). \$ $p \leq 0.05$ versus Control without IGF-1 (Aspin–Welch test).

medium for 3 days in the absence or presence of IGF-1 and 8, and the neuronal survival rate was estimated on the basis of βIII-tubulin immunoreactivities. Under this condition, IGF-1 alone exhibited a significant but weak increase (up to 1.3-fold at

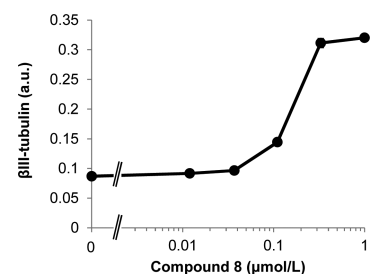


Figure 3. Dose-dependent neuroprotective effect of 8 in rat primary neural cells. Cells were treated with 100 ng/mL IGF-1 and 8 as described in Figure 2. In the presence of IGF-1, 8 increased βIII-tubulin immunoreactivities in a concentration-dependent manner. EC₅₀ value was 0.15 μmol/L (95% confidence interval is 0.13–0.20 μmol/L). A four-parameter logistic model was used to calculate the EC₅₀ value. Data represent mean ± SEM of four wells.

10 ng/mL) in neuronal survivability. This effect was observed to be concentration-independent in the concentration range from 3 to 100 ng/mL. Compound **8** (1 $\mu\text{mol/L}$) alone increased the neuronal survival rate 3-fold compared with that of the control; in addition, in the presence of 1 $\mu\text{mol/L}$ of **8**, depending on the concentration, IGF-1 enhanced the neuroprotective effect by approximately 6-fold (main effect of **8**, $p \leq 0.05$; main effect of IGF-1, $p \leq 0.05$; interaction of compound **8** and IGF-1, $p \leq 0.05$ (two-way ANOVA)) (Figure 2). In contrast, in the presence of 100 ng/mL of IGF-1, which is a concentration relevant to physiological conditions, **8** increased the neuronal survival rate in a concentration-dependent manner, with an EC_{50} value of 0.15 μM ; this effect plateaued at 0.33 μM , where the neuronal survival rate increased approximately 3-fold (Figure 3). In conclusion, treatment with IGF-1 or **8** induced a 1.3- or 3-fold increase in the neuronal survival rate, respectively, and cotreatment further enhanced it as much as 6-fold. These results clearly demonstrate that, although IGF-1 and **8** individually exhibit the neuroprotective effect, they act in a collaborative manner to produce greater neuroprotective activity.

We have not yet elucidated how these compounds interact with the IGF-1 signaling to sensitize the cells to IGF-1. Although the underlying mechanism needs to be clarified, exploring the pharmacological effects of the "IGF-1 sensitizer" in vivo would be interesting. For this purpose, **8** was selected as an appropriate chemical probe among the three potent compounds **8**, **13e**, and **18j** because **13e** exhibited a faster metabolic clearance than **8** (**8**, 2 $\mu\text{L}/\text{min}/\text{mg}$; **13e**, 30 $\mu\text{L}/\text{min}/\text{mg}$) and **18j** caused a slight decrease in cellular ATP content at 100 μM in a general cytotoxicity assay (**8**, 93.3%; **18j**, 68.0%). Moreover, **8** has been observed to be brain-penetrable in rats (K_p was 2.9 at 1 h after iv administration). At present, **8** is being evaluated in several in vivo tests, including disease models, to search for possible indications of an "IGF-1 sensitizer."

CONCLUSION

A series of benzofuran derivatives with neuroprotective activity based on their collaborative effect with IGF-1 was discovered. Among the three scaffolds tested, 2,3-dihydro-1-benzofuran derivatives exhibited potent activity without any adverse effects such as CYP2C9 inhibition or photoinduced cytotoxicity. A subsequent SAR study of the dihydrobenzofuran derivatives revealed (1) an advantage of lipophilic substituents at the 2-position, (2) the importance of the molecular framework defined by the linker, and (3) the effect of the substituent on the terminal aryl ring. As a result, we observed **8**, as a representative compound, to exhibit potent neuroprotective activity with brain penetrability. An in vitro pharmacological study demonstrated that, although IGF-1 and **8** individually exhibited neuroprotective effects, **8** acted in collaboration with IGF-1 to exhibit greater neuroprotective activity. Compound **8** is being evaluated in several tests to explore its potential therapeutic applications; the results of the pharmacological characterization and mechanistic study will be reported elsewhere.

EXPERIMENTAL SECTION

1-(4-Methoxyphenyl)-4-(2,2,4,6,7-pentamethyl-2,3-dihydro-1-benzofuran-5-yl)piperazine (8). To an ice-cooled suspension of LiAlH_4 (577 mg, 15.2 mmol) in THF (20 mL) was added AlCl_3 (2.03 g, 15.2 mmol). After stirring at 0 $^\circ\text{C}$ for 10 min, a solution of **1a** (2.00 g, 5.07 mmol) in THF (25 mL) was added and the mixture was

refluxed with stirring for 2 h. After cooling, water and 0.5 M NaOH were added to the mixture. The mixture was stirred at rt for 1 h and extracted with EtOAc. The extract was washed with satd NaCl, dried over MgSO_4 , and concentrated under reduced pressure. The residue was purified by silica gel chromatography (hexane–EtOAc, 90:10 to 75:25) and successively recrystallized from EtOAc/hexane to give the title compound (1.60 g, 83%) as colorless crystals; mp 152–155 $^\circ\text{C}$. $^1\text{H NMR}$ (CDCl_3): δ 1.46 (6H, s), 2.08 (3H, s), 2.19 (3H, s), 2.24 (3H, s), 2.91 (2H, s), 3.06–3.34 (8H, m), 3.78 (3H, s), 6.81–6.90 (2H, m), 6.92–7.01 (2H, m). ESI MS m/z 381 $[\text{M} + \text{H}]^+$. Anal. Calcd for $\text{C}_{24}\text{H}_{32}\text{N}_2\text{O}_2$: C, 75.75; H, 8.48; N, 7.36. Found: C, 75.50; H, 8.52; N, 7.15.

ASSOCIATED CONTENT

Supporting Information

The Supporting Information is available free of charge on the ACS Publications website at DOI: 10.1021/acs.jmedchem.6b00191.

Experimental information and methods; chemistry, ADME-tox, and PK studies; biology (PDF)
Molecular formula strings (CSV)

AUTHOR INFORMATION

Corresponding Author

*Phone: +81-466-32-1284. Fax: +81-466-29-4451. E-mail: takeshi.wakabayashi@takeda.com.

Notes

The authors declare no competing financial interest.

ACKNOWLEDGMENTS

We are grateful to Dr. Shigenori Ohkawa and Masahiro Okura for their pioneering works on this research. We thank Yasuhiko Kawano and Akihisa Maeda for their support with the synthesis, Dr. Hideo Fujiwara, Masahiko Hattori, and Masumi Sagayama for their support with the biological experiments, Keiko Higashikawa and Mitsuyoshi Nishitani for their assistance with the X-ray measurements, and Dr. Shinji Fujimoto, Akira Oda, and Yuhei Miyanoana for their valuable discussions. Drs. Takanobu Kuroita and Takashi Miki are also acknowledged for their guidance and for proofreading of the manuscript.

ABBREVIATIONS USED

DMF, *N,N*-dimethylformamide; EtOAc, ethyl acetate; EtOH, ethanol; *KOt*-Bu, potassium *tert*-butoxide; MeCN, acetonitrile; MEK, methyl ethyl ketone; *NaOt*-Bu, sodium *tert*-butoxide; Pd/C, palladium on carbon; PhNEt₂, diethylaniline; rt, room temperature; TFA, trifluoroacetic acid; THF, tetrahydrofuran

REFERENCES

- (1) Laron, Z. Insulin-like growth factor 1 (IGF-1): a growth hormone. *Mol. Pathol.* **2001**, *54*, 311–316.
- (2) Plum, L.; Schubert, M.; Brüning, J. C. The role of insulin receptor signaling in the brain. *Trends Endocrinol. Metab.* **2005**, *16*, 59–65.
- (3) Torres-Aleman, I. Serum growth factors and neuroprotective surveillance. *Mol. Neurobiol.* **2001**, *21*, 153–160.
- (4) Gasparini, L.; Xu, H. Potential roles of insulin and IGF-1 in Alzheimer's disease. *Trends Neurosci.* **2003**, *26*, 404–406.
- (5) DiCicco-Bloom, E.; Black, I. B. Insulin growth factors regulate the mitotic cycle in cultured rat sympathetic neuroblasts. *Proc. Natl. Acad. Sci. U. S. A.* **1988**, *85*, 4066–4070.
- (6) Guan, J.; Williams, C.; Gunning, M.; Mallard, C.; Gluckman, P. The effects of IGF-1 treatment after hypoxic-ischemic brain injury in adult rats. *J. Cereb. Blood Flow Metab.* **1993**, *13*, 609–616.

(7) McMorris, F. A.; Dubois-Dalcq, M. Insulin-like growth factor I promotes cell proliferation and oligodendroglial commitment in rat glial progenitor cells developing in vitro. *J. Neurosci. Res.* **1988**, *21*, 199–209.

(8) Lenoir, D.; Honegger, P. Insulin-like growth factor I (IGF I) stimulates DNA synthesis in fetal rat brain cell cultures. *Dev. Brain Res.* **1983**, *7*, 205–213.

(9) Kimpinski, K.; Mearow, K. Neurite growth promotion by nerve growth factor and insulin-like growth factor-1 in cultured adult sensory neurons: Role of phosphoinositide 3-kinase and mitogen activated protein kinase. *J. Neurosci. Res.* **2001**, *63*, 486–499.

(10) Guthrie, K. M.; Nguyen, T.; Gall, C. M. Insulin-like growth factor-1 mRNA is increased in deafferented hippocampus: spatiotemporal correspondence of a trophic event with axon sprouting. *J. Comp. Neurol.* **1995**, *352*, 147–160.

(11) Nilsson, L.; Sara, V.; Nordberg, A. Insulin-like growth factor 1 stimulates the release of acetylcholine from rat cortical slices. *Neurosci. Lett.* **1988**, *88*, 221–226.

(12) Hong, M.; Lee, V.M.-Y. Insulin and insulin-like growth factor-1 regulate tau phosphorylation in cultured human neurons. *J. Biol. Chem.* **1997**, *272*, 19547–19553.

(13) Dore, S.; Bastianetto, S.; Kar, S.; Quirion, R. Protective and rescuing abilities of IGF-I and some putative free radical scavengers against β -amyloid-inducing toxicity in neurons. *Ann. N. Y. Acad. Sci.* **1999**, *890*, 356–364.

(14) Pajouhesh, H.; Lenz, G. R. Medicinal chemical properties of successful central nervous system drugs. *NeuroRx* **2005**, *2*, 541–553.

(15) Davis, R. D.; Fitzgerald, R. N.; Guo, J. Improved method for the synthesis of 2-methyl-2-aryloxypropanoic acid derivatives. *Synthesis* **2004**, *12*, 1959–1962.

(16) Diedrichs, N.; Ragot, J. P.; Thede, K. A highly efficient synthesis of rocaglaols by a novel α -arylation of ketones. *Eur. J. Org. Chem.* **2005**, *2005*, 1731–1735.

(17) Ohkawa, S.; Fukatsu, K.; Miki, S.; Hashimoto, T.; Sakamoto, J.; Doi, T.; Nagai, Y.; Aono, T. 5-Aminocoumarans: dual inhibitors of lipid peroxidation and dopamine release with protective effects against central nervous system trauma and ischemia. *J. Med. Chem.* **1997**, *40*, 559–573.

(18) Cruciani, G.; Carosati, E.; De Boeck, B.; Ethirajulu, K.; Mackie, C.; Howe, T.; Vianello, R. MetaSite: understanding metabolism in human cytochromes from the perspective of the chemist. *J. Med. Chem.* **2005**, *48*, 6970–6979.

(19) Smith, G. F. Designing drugs to avoid toxicity. *Prog. Med. Chem.* **2011**, *50*, 1–47.

(20) Peters, B.; Holzhütter, H.-G. In vitro phototoxicity testing: development and validation of a new concentration response analysis software and biostatistical analyses related to the use of various prediction models. *ATLA, Altern. Lab. Anim.* **2002**, *30*, 415–432.

(21) Veber, D. F.; Johnson, S. R.; Cheng, H.-Y.; Smith, B. R.; Ward, K. W.; Kopple, K. D. Molecular properties that influence the oral bioavailability of drug candidates. *J. Med. Chem.* **2002**, *45*, 2615–2623.